Inorg. Chem. **2005**, *44*, 4834–4842

Inorganic Chemistry
Article

Reactions of Methane with Titanium Atoms: CH_3TiH, $CH_2{=}TiH_2$, Agostic Bonding, and $(CH_3)_2TiH_2$

Lester Andrews,* Han-Gook Cho, and Xuefeng Wang

Department of Chemistry, University of Virginia, P.O. Box 400319,
Charlottesville, Virginia 22904-4319

Received February 18, 2005

Laser-ablated titanium atoms react with methane to form the insertion product CH_3TiH, which undergoes a reversible photochemical α-H transfer to give the methylidene complex $CH_2{=}TiH_2$. On annealing a second methane activation occurs to produce $(CH_3)_2TiH_2$. These molecules are identified from matrix infrared spectra by isotopic substitution (CH_4, $^{13}CH_4$, CD_4, CH_2D_2) and comparison to DFT frequency calculations. The computed planar structure for singlet ground-state $CH_2{=}TiH_2$ shows CH_2 distortion and evidence for agostic bonding (H–C–Ti, 91.4°), which is supported by the spectra for $CHD{=}TiHD$.

Introduction

Transition metal complexes containing carbon−metal double bonds are important for understanding metal−carbon interactions and for developing catalysts for use in methane activation and initiators for alkene metathesis reactions.[1,2] The activation of methane by transition-metal catalyst systems is important for the synthesis of useful chemicals.

A number of early transition-metal alkylidene complexes show evidence of agostic bonding, and these systems provide a basis to characterize the agostic interaction.[1] The simplest compound of this type is the metal methylidene dihydride complex, $CH_2{=}MH_2$, which is an ideal model system to examine substituent effects and the agostic interaction.[3−5] Such Schrock-type carbenes have been investigated by early electronic structure calculations using minimum basis sets which found stable symmetrical structures with no agostic interaction.[6] More recent MC/LMO/CI and MCSCF computations in C_{2v} symmetry also gave a stable $CH_2{=}TiH_2$ structure.[7] Recently, we have reacted Zr atoms with CH_4 and prepared $CH_2{=}ZrH_2$ for infrared spectroscopic investigation: the observed frequencies match those calculated for a distorted, agostic $CH_2{=}ZrH_2$ molecule including the $CHD{=}ZrHD$ isotopic molecules, which show inequivalent H(D) atoms on the metal center.[8] Similar evidence has been obtained very recently for $CH_2{=}HfH_2$.[9]

Methyl halides are more reactive with electron deficient group 4 transition metal atoms than CH_4, and several $CH_2{=}MHX$ methylidene compounds have been prepared and their structures computed. We find that the agostic interaction increases in the series $CH_2{=}TiHX$ (X = F, Cl, Br) but decreases in the series $CH_2{=}MHF$ (M = Ti, Zr, Hf).[10−13] These systems also activate a second CH_4 or CH_3X molecule to form $(CH_3)_2ZrH_2$, $(CH_3)_2TiF_2$, $(CH_3)_2TiCl_2$, and $(CH_3)_2TiBr_2$.[10,13,14] The $(CH_3)_2TiCl_2$ compound has been prepared and investigated separately.[15] Therefore, we expect the $(CH_3)_2TiH_2$ molecule to be stable.

Recently, thermally evaporated Ti atoms have been found unreactive with CH_4 in excess argon. However, visible

---

* Author to whom correspondence should be addressed. E-mail: lsa@virginia.edu.

(1) Schrock, R. R. *Chem. Rev.* **2002**, *102*, 145.
(2) Buchmeiser, M. R. *Chem. Rev.* **2000**, *100*, 1565.
(3) Crabtree, R. H. *Chem. Rev.* **1985**, *85*, 245.
(4) Ujaque, G.; Cooper, A. C.; Maseras, F.; Eisenstein, O.; Caulton, K. G. *J. Am. Chem. Soc.* **1998**, *120*, 361.
(5) Wada, K.; Craig, B.; Pamplin, C. B.; Legzdins, P.; Patrick, B. O.; Tsyba, I.; Bau, R. *J. Am. Chem. Soc.* **2003**, *125*, 7035.
(6) (a) Franci, M. M.; Pietro, W. J.; Hout, R. F., Jr.; Hehre, W. J. *Organometallics* **1983**, *2*, 281. (b) Franci, M. M.; Pietro, W. J.; Hout, R. F., Jr.; Hehre, W. J. *Organometallics* **1983**, *2*, 815.
(7) (a) Cundari, T. R.; Gordon, M. S. *J. Am. Chem. Soc*. **1992**, *114*, 539. (b) Chung, G.; Gordon, M. S. *Organometallics* **2003**, *22*, 42.
(8) Cho, H.-G.; Wang, X.; Andrews, L. *J. Am. Chem. Soc.* **2005**, *127*, 465.
(9) Cho, H.-G.; Wang, X.; Andrews, L. *Organometallics*, **2005**, om050069l, in press.
(10) Cho, H.-G.; Andrews, L. *J. Phys. Chem. A* **2004**, *108*, 6294.
(11) Cho, H.-G.; Andrews, L. *J. Am. Chem. Soc.* **2004**, *126*, 10485.
(12) Cho, H.-G.; Andrews, L. *Organometallics* **2004**, *23*, 4357.
(13) Cho, H.-G.; Andrews, L. *Inorg. Chem.* **2005**, *44*, 979.
(14) Cho, H.-G.; Andrews, L. *Inorg. Chem.* **2004**, *43*, 5253.
(15) McGrady, G. S.; Downs, A. J.; Bednall, N. C.; McKean, D. C.; Thiel, W.; Jonas, V.; Frenking, G.; Scherer, W. *J. Phys. Chem. A* **1997**, *101*, 1951 and references therein.

10.1021/ic0502574 CCC: $30.25

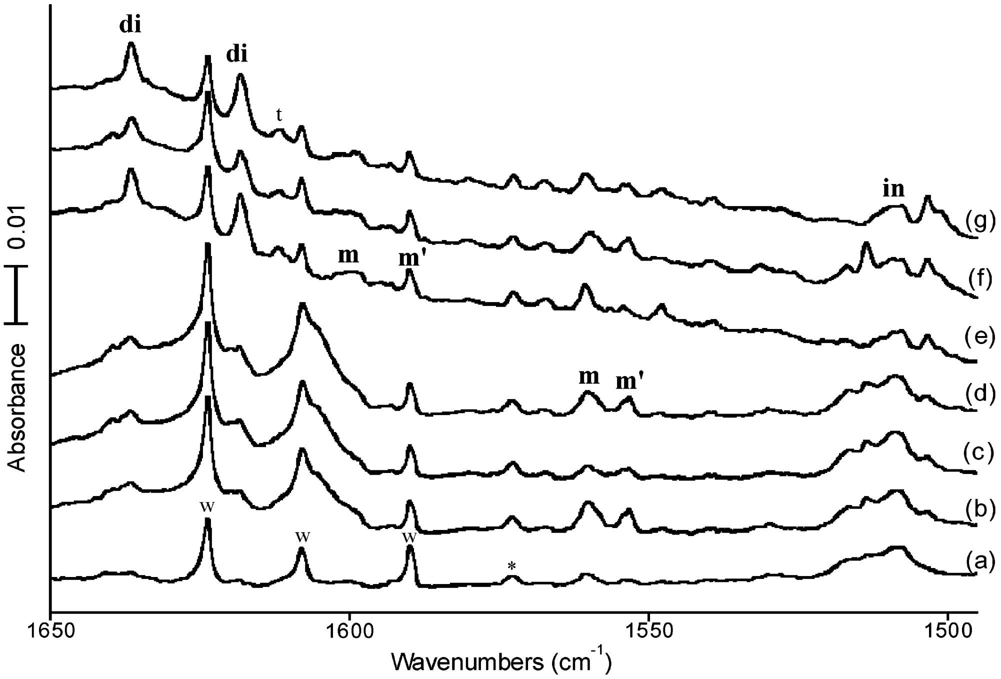

Figure 1. Infrared spectra in the 1650−1495 cm^{-1} region for the products of reactions of laser-ablated Ti atoms and CH_4 in argon at 8 K: (a) Ti + 1% CH_4 in Ar codeposited for 60 min; (b) after 290−380 nm irradiation for 20 min; (c) after $\lambda > 420$ nm irradiation; (d) after 290−380 nm irradiation for 20 min; (e) after annealing to 26 K; (f) after 240−380 nm irradiation; (g) after annealing to 26 K. W denotes water, and $*$ denotes common absorptions.

photoexcitation of titanium led to a new absorption at 1513.5 cm^{-1} identified as the CH_3TiH insertion product.[16] We also prepare this molecule and perform selective photochemistry, which promotes α-hydrogen transfer to form the methylidene dihydride $CH_2{=}TiH_2$, and sample annealing, which produces the new $(CH_3)_2TiH_2$ molecule. The results of our experiments and electronic structure calculations will be reported here.

Experimental and Computational Methods

The laser-ablation matrix-infrared experiment has been described previously.[17,18] Briefly, laser-ablated titanium atoms (Goodfellow) were reacted with CH_4 (Matheson, UHP grade), $^{13}CH_4$, CD_4, and CH_2D_2 (Cambridge Isotopic Laboratories) in excess neon (Spectra Gases) or argon (MG Industries) during condensation on a CsI window at 4 or 8 K. Infrared spectra were recorded at 0.5 cm^{-1} resolution on Nicolet Magna spectrometers with HgCdTe type B detectors. Samples were irradiated by a mercury arc lamp (175 W, globe removed) using optical filters for 20 min periods and annealed, and more spectra were recorded.

Complementary density functional theory (DFT) calculations were done using the Gaussian 98 package,[19] the B3LYP density functional,[20] and the all-electron medium 6-311++G(2d, p) and large 6-311++G(3df, 3pd) basis sets with the specified polarization functions on C, Ti, and H, respectively,[21] to provide a consistent set of vibrational frequencies for the reaction products. The SDD effective core potential (12 valence electrons)[22] and basis set was used for Ti in the largest product molecule because of limited computer storage space. Geometries were fully relaxed during optimization, the optimized geometry was confirmed via vibrational analysis, and the vibrational frequencies were calculated analytically.

Results

Experiments with Ti and CH_4 in excess argon and neon and DFT calculations of expected reaction products will be presented.

Argon Matrix. A series of experiments was performed reacting 0.5, 1.0, and 2.0% CH_4 in argon with laser-ablated Ti atoms, and infrared spectra from the 1% CH_4 investigation are shown in Figure 1. The major new product absorption at 1508.7 cm^{-1} is in a group of bands labeled **in**, a weak new absorption labeled **m** is observed at 1560.0 cm^{-1}, with a weaker associated band at 1598.1 cm^{-1}, and very weak

---

(16) Bihlmeier, A.; Greene, T. M.; Himmel, H.-J. *Organometallics* **2004**, *23*, 2350.

(17) Chertihin, G. V.; Andrews, L. *J. Phys. Chem.* **1995**, *99*, 6356 (TiO_2).

(18) Andrews, L.; Citra, A. *Chem. Rev.* **2002**, *102,* 885 and references therein.

(19) Frisch, M. J.; Trucks, G. W.; Schlegel, H. B.; Scuseria, G. E.; Robb, M. A.; Cheeseman, J. R.; Zakrzewski, V. G.; Montgomery, J. A., Jr.; Stratmann, R. E.; Burant, J. C.; Dapprich, S.; Millam, J. M.; Daniels, A. D.; Kudin, K. N.; Strain, M. C.; Farkas, O.; Tomasi, J.; Barone, V.; Cossi, M.; Cammi, R.; Mennucci, B.; Pomelli C.,; Adamo, C.; Clifford, S.; Ochterski, J.; Petersson, G. A.; Ayala, P. Y.; Cui, Q.; Morokuma, K.; Rega, N.; Salvador, P.; Dannenberg, J. J.; Malick, D. K.; Rabuck, A. D.; Raghavachari, K.; Foresman, J. B.; Cioslowski, J.; J. V. Ortiz,; Baboul, A. G.; Stefanov, B. B.; Liu, G.; Liashenko, A.; Piskorz, P.; Komaromi, I.; Gomperts, R.; Martin, R. L.; Fox, D. J.; Keith, T.; Al-Laham, M. A.; Peng, C. Y.; Nanayakkara, A.; Challacombe, M.; Gill, P. M. W.; Johnson, B.; Chen, W.; Wong, M. W.; Andres, J. L.; Gonzalez, C.; Head-Gordon, M.; Replogle, E. S.; Pople, J. A. *Gaussian 98*, revision A.11.4; Gaussian, Inc.: Pittsburgh, PA, 2002.

(20) (a) Becke, A. D. *J. Chem. Phys.* **1993**, *98*, 5648. (b) Lee, C.; Yang, E.; Parr, R. G. *Phys. Rev. B* **1988**, *37*, 785. (c) Stevens, P. J.; Devlin, F. J.; Chablowski, C. F.; Frisch, M. J. *J. Phys. Chem.* **1994**, *98*, 11623.

(21) (a) Krishnan, R.; Binkley, J. S.; Seeger, R.; Pople, J. A. *J. Chem. Phys.* **1980**, *72*, 650. (b) Frisch, M. J.; Pople, J. A.; Binkley, J. S. *J. Chem. Phys.* **1984**, *80*, 3265.

(22) Andrae, D.; Haeussermann, U.; Dolg, M.; Stoll, H.; Preuss, H. *Theor. Chim. Acta* **1990**, *7*, 123.

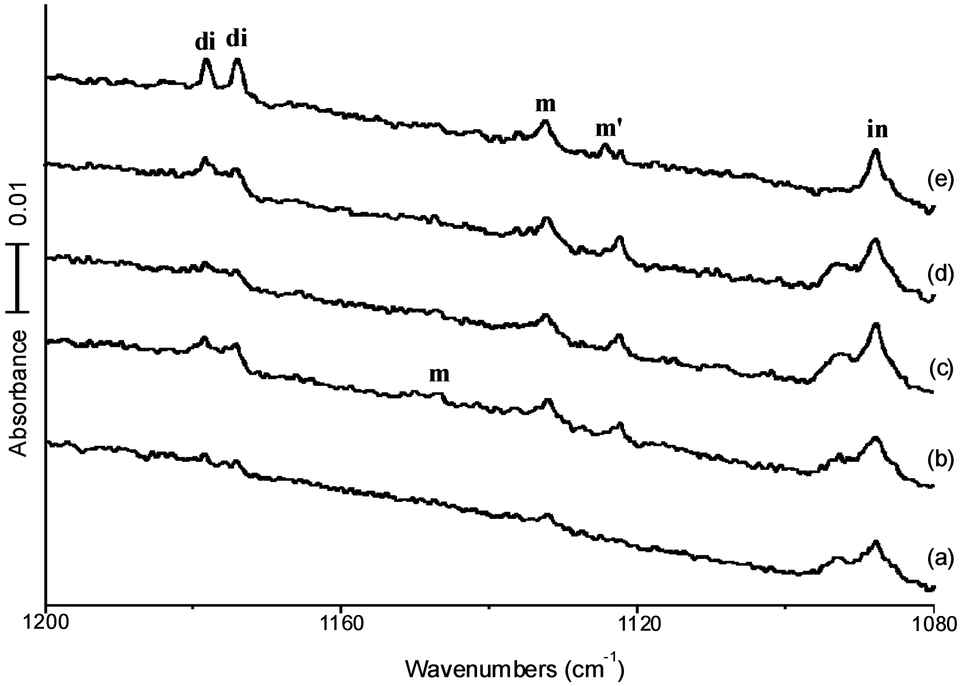

Figure 2. Infrared spectra in the 1200−1080 cm^{-1} region for the products of reactions of laser-ablated Ti atoms and CD_4 in argon at 8 K: (a) Ti + 2% CD_4 in Ar codeposited for 60 min; (b) after $\lambda > 290$ nm irradiation for 20 min; (c) after $\lambda > 420$ nm irradiation; (d) after 290−380 nm irradiation; (e) after annealing to 26 K.

bands labeled **di** are observed at 1636.5 and 1618.2 cm^{-1}. Irradiation in the near-ultraviolet at 290−380 nm markedly increased the **m** (1560.0 cm^{-1}) and **m′** (1553.1 cm^{-1}) bands and slightly increased the **di** and **in** bands (Figure 1b). Subsequent irradiation in the visible at $\lambda > 420$ nm reduced the **m** bands by 70%, increased the **in** group by 20%, and doubled the **di** bands. The next 290−380 nm irradiation doubled the **m** group, left the **di** pair unaffected, and decreased the **in** group by 15% (Figure 1d). Annealing to 26 K markedly increased the **di** pair of absorptions and slightly decreased the other two groups (Figure 1e). The very weak band at 1611.8 cm^{-1} (marked t) is the strongest band for H_2TiO in the Ti/H_2O system.[23] In addition very weak TiO_2 bands[17] are observed. A subsequent 240−380 nm irradiation halved the **di** bands but increased **m** and **in** bands (including the matrix trapping sites at 1516.8, 1513.5, and 1503.3 cm^{-1}). Another annealing to 26 K (Figure 1g) had the same effect as before. Subsequent irradiations at $\lambda > 420$ nm and at 290−380 nm (not shown) also had the same effect as described above. Additional absorptions at 653.7 cm^{-1} tracked photochemically with the **m** group and at 588.5 cm^{-1} followed the **di** pair: the methyl radical band profile at 617 and 603 cm^{-1} decreased on annealing.[24] Although an increasing CH_4 concentration slightly increased the absolute **m** and **in** band intensities, they maintained the same relative intensity; however, the **di** band yield increased markedly relative to the **m** and **in** groups with increasing CH_4 concentration.

Isotopic substitution of the methane precursor was employed. Two CD_4 experiments were done, and spectra from the higher concentration sample are shown in Figure 2. Again the **in** band system at 1088.2 cm^{-1} is the major deposition product and ultraviolet irradiation slightly increased the **in** bands and increased the **di** bands at 1178.5 and 1174.2 cm^{-1} and the **m** bands at 1147.3, 1132.2, and 1122.2 cm^{-1} even more: a weaker associated **m** band was found at 514.0 cm^{-1}. As before visible ($\lambda > 420$ nm) irradiation slightly decreased the **m** in favor of the **in** bands, and near-ultraviolet (290−380 nm) irradiation reversed this change. Finally, annealing to 26 K markedly increased the **di** bands and produced a weaker associated 510.0 cm^{-1} band. The observed frequencies are collected in Table 1.

Investigations with the CH_2D_2 precursor provided diagnostic information, and spectra are illustrated in Figure 3. The **in** band system at 1508 cm^{-1} is essentially unchanged from CH_4, but the CD_4 counterpart is masked by strong CH_2D_2 absorption. There are, however, differences in the **di** and **m** band systems. Weak **m** bands are observed at 1560.0 and 1553.5 cm^{-1} with stronger counterparts at 1573.0 and 1566.8 cm^{-1} with deuterium counterparts at 1132.9, 1137.3, and 1143.6 cm^{-1}. Arrows mark the new mixed isotopic **m** bands in Figure 3. The **di** bands now appear at 1636.7 and 1618.1 cm^{-1} with a new stronger intermediate component at 1627.2 cm^{-1} and at 1179.4 and 1173.9 cm^{-1} with a weaker intermediate component at 1176.7 cm^{-1}.

One experiment was done with 0.5% $^{13}CH_4$, and the stronger **di**, **m**, and **in** bands were observed unshifted from the $^{12}CH_4$ product frequencies.

Neon Matrix. A similar set of investigations was performed in excess neon, and representative spectra are shown in Figure 4. Neon condensing at 4 K does not isolate CH_4 as well as argon condensing at 8 K, and as a result, product absorptions are broader in solid neon and the **di** bands are

---

(23) Zhou, M. F.; Zhang, L.; Dong, J.; Qin, Q. *J. Am. Chem. Soc.* **2000**, *122*, 10680.

(24) Jacox, M. E. *J. Mol. Spectrosc.* **1977**, *66*, 272.

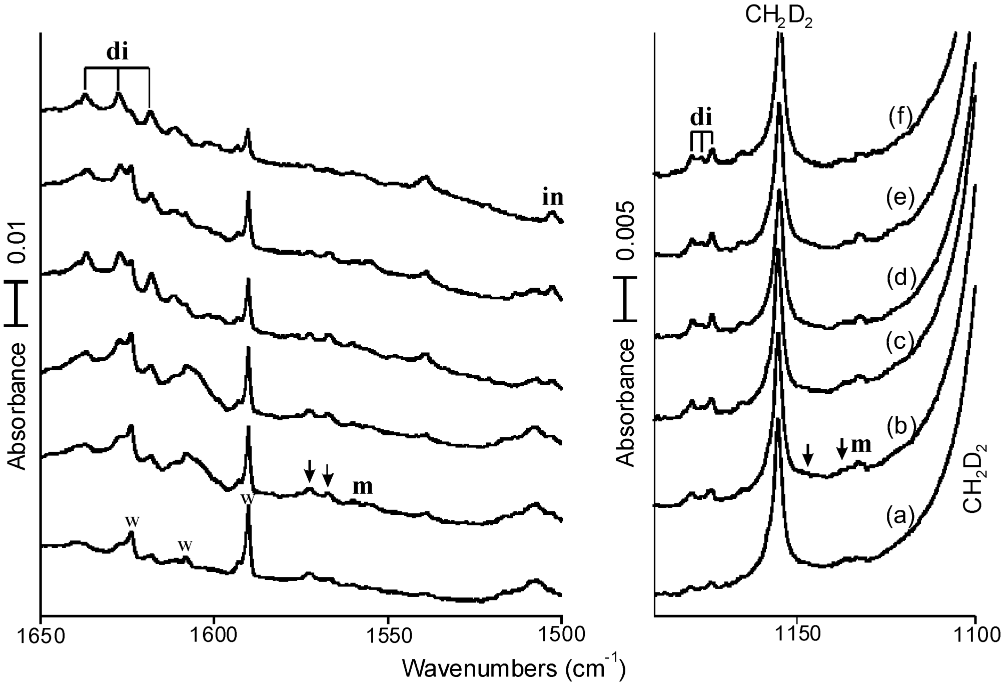

Figure 3. Infrared spectra in the 1650−1500 and 1190−1100 cm^{-1} regions for the products of reactions of laser-ablated Ti atoms and CH_2D_2 in argon at 8 K: (a) Ti + 2% CH_2D_2 in Ar codeposited for 60 min; (b) after 290−380 nm irradiation for 20 min; (c) after λ > 420 nm irradiation; (d) after annealing to 26 K; (e) after 240−380 nm irradiation; (f) after annealing to 32 K.

Table 1. Infrared Absorptions (cm^{-1}) Observed from Reactions of Titanium Atoms and Methane

matrix	CH_4	$^{13}CH_4$	CH_2D_2	CD_4	identification
argon	1636.5	1636.5	1636.7, 1179.4	1178.5	**di**, $(CH_3)_2TiH_2$
			1627.2, 1176.7		**di**, Me_2TiHD
	1618.2	1618.2	1618.1, 1173.9	1174.2	**di**, $(CH_3)_2TiH_2$
	1598.1		1573.0, 1143.6	1147.3	**m**, $CH_2{=}TiH_2$
	1594.4		1566.8, 1137.3		**m**, $CH_2{=}TiH_2$
	1560.0	1560.0	1560.0, 1132.9	1132.2	**m**, $CH_2{=}TiH_2$
	1553.1	1553.1	1555.3	1122.2	**m**, $CH_2{=}TiH_2$
	1516.8	1516.8	1517, masked[a]	1093.4	**in**, CH_3TiH
	1513.5	1513.5	1513, masked	1092.2	**in**, CH_3TiH
	1508.7	1508.7	1509, masked	1088.2	**in**, CH_3TiH
	1503.3	1503.3	1503, masked		**in**, CH_3TiH
	635.7			514.0	**m**, $CH_2{=}TiH_2$
	617,603	612, 598			CH_3
	588.5			510.0	**di**, $(CH_3)_2TiH_2$
neon	1657	1657			**di**, $(CH_3)_2TiH_2$
			1647, 1191		**di**, $(CH_3)_2TiH_2$
	1637	1637		1188	**di**, $(CH_3)_2TiH_2$
	1606.4	1606.4	1626.0, 1606.4, 1175.0, 1164.0	1164.0	
	1541.4	1541.4	1540.9, 1111.5	1111.4	**in**, CH_3TiH
	1540	1540	1540, 1111	1110	**in**, CH_3TiH
	1453.5	1453.5	1462.3, 1055.0	1047.3	**h**, $TiH_2(C_2H_6)$
	612	608			CH_3
	593.0	588.5		513.6	**di**, $(CH_3)_2TiH_2$

[a] Deuterium counterpart is masked by precursor absorption.

formed directly on irradiation before annealing. The major product on sample deposition at 1540 cm^{-1} is marked **in**. Visible irradiation (λ > 470 nm) decreased the latter band, but ultraviolet (240−380 nm) light restored the band and produced strong new 1657 and 1637 cm^{-1} **di** absorptions and new 1456 and 1437 cm^{-1} **h** bands (Figure 4c). A second visible irradiation (λ > 530 nm) with less energetic photons also reduced the 1540 cm^{-1} band (not shown), and annealing to 10 K sharpened the broader features to 1541.4 and 1453.5 cm^{-1} (labeled **in** and **h**) and produced structure on the **di** bands (Figure 4d). Subsequent ultraviolet irradiation (240−380 nm) restored the broad **h**, **in**, and **di** bands, and annealing reproduced the sharp peaks. In the lower region a weak 593.0 cm^{-1} band behaved as the **di** bands, and a 612 cm^{-1} feature which disappeared on annealing is probably due to the methyl radical.

Isotopically substituted methane samples were employed. The $^{13}CH_4$ reagent gave the same upper bands, and the lower bands shifted to 588.5, 608, and 1318.5 cm^{-1}. The CD_4 precursor gave one broad **di** band at 1188 cm^{-1} and a

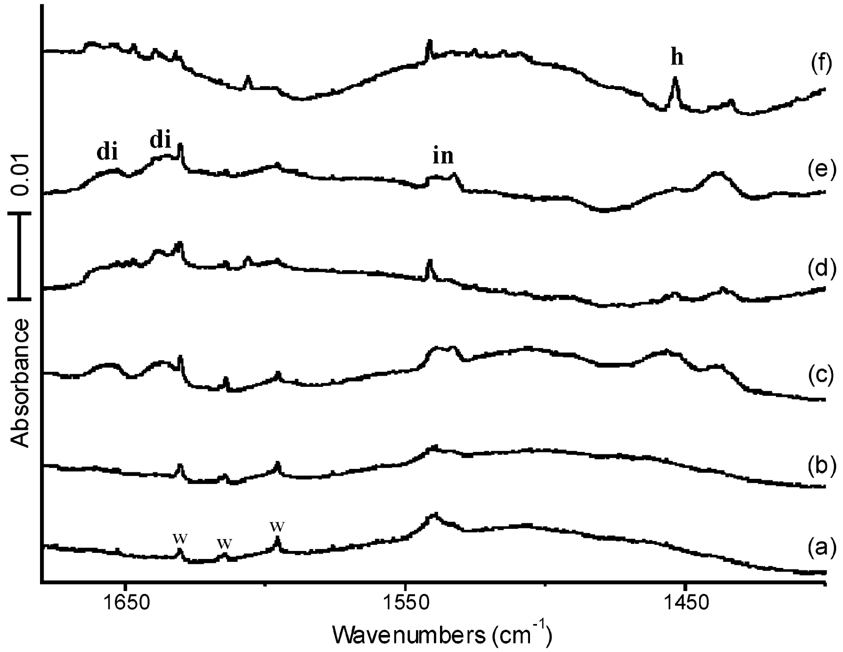

Figure 4. Infrared spectra in the 1680−1400 cm^{-1} region for the products of reactions of laser-ablated Ti atoms and CH_4 in neon at 4 K: (a) Ti + 1% CH_4 in Ne codeposited for 60 min; (b) after $\lambda > 470$ nm irradiation for 20 min; (c) after 240−380 nm irradiation; (d) after annealing to 10 K; (e) after 240−380 nm irradiation; (f) after annealing to 13 K.

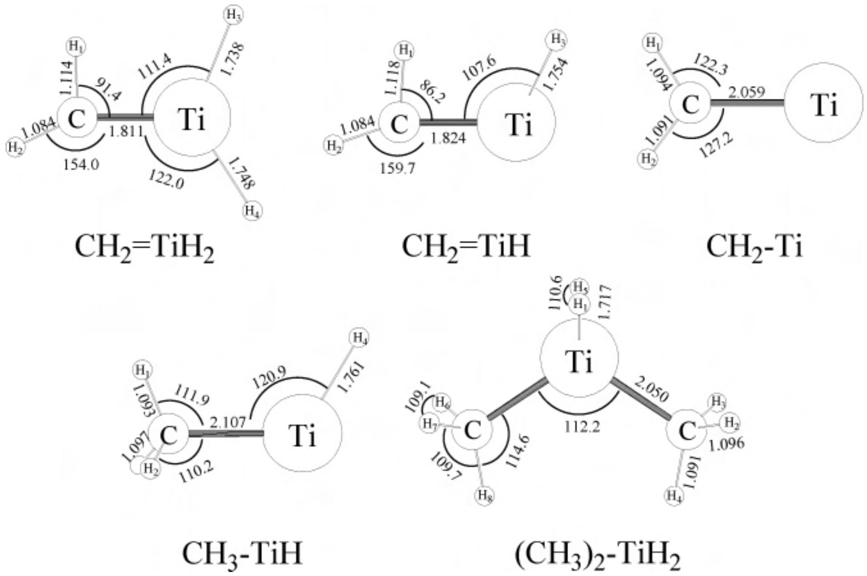

Figure 5. Structures of ground-state C, H, and Ti species calculated at the B3LYP all-electron 6-311++G(3df,3pd) level.

1110 cm^{-1} **in** feature, which sharpened to 1111.4 cm^{-1} on annealing, and a weak 513.6 cm^{-1} **di** band. The CH_2D_2 reagent produced broad **di** bands at 1647 and 1191 cm^{-1} and **in** features which sharpened to 1540.9 and 1111.5 cm^{-1} on annealing. In addition, broad **h** bands at 1461 and 1054 cm^{-1} sharpened to 1462.3 and 1055.0 cm^{-1} on annealing.

Calculations. DFT computations were done at the B3LYP level using both all-electron medium 6-311++G(2d,p) and large 6-311++G(3df,3pd) basis sets for anticipated product molecules. The structures illustrated in Figure 5 using the large basis set include the $CH_2{=}TiH$ radical and the triplet ground-state $CH_2{=}Ti$ species for comparison with the expected $CH_2{=}TiH_2$, CH_3TiH, and $(CH_3)_2TiH_2$ products of Ti and CH_4 reactions. The medium basis set gave slightly different bond lengths (Ti−C, 2.052 Å; Ti−H, 1.716 Å) for the singlet ground-state $(CH_3)_2TiH_2$ with C_2 symmetry.

The frequencies computed for singlet $CH_2{=}TiH_2$ are listed in Table 2 for all-electron calculations using the medium and large basis sets. The frequencies are slightly higher, the C═Ti bond is slightly longer (1.814 Å), the Ti−H bonds are slightly longer (1.740, 1.749 Å), and the agostic H−C−Ti angle is slightly larger (91.9°) for the medium basis set calculation. Note that polarization functions on carbon[4,8,9] are required to characterize agostic distortion. Using the large basis set for C and H and the SDD pseudopotential for Ti gave almost the same distorted structure (C═Ti, 1.806 Å; agostic angle 91.6°). The triplet $CH_2{-}TiH_2$ state is

Table 2. Harmonic Vibrational Frequencies (cm^{-1}) Computed for the C_s Singlet Ground-State Structure of $CH_2{=}TiH_2$ Using Medium and Large Basis Sets and the B3LYP Density Functional

	$^{12}CH_2{=}TiH_2$		$^{12}CH_2{=}TiH_2$		$^{13}CH_2{=}TiH_2$		$CD_2{=}TiD_2$	
mode	freq[a]	int[b]	freq[c]	int[b]	freq[c]	int[b]	freq[c]	int[b]
CH_2 str	3182.7	1	3173.4	1	3162.5	1	2349.6	2
CH_2 str	2868.3	2	2764.5	2	2858.0	2	2083.6	1
TiH_2 str	1673.5	262	1673.6	372	1673.6	372	1191.3	204
TiH_2 str	1631.7	643	1629.9	672	1529.9	672	1171.8	353
CH_2 bend	1315.2	16	1316.2	17	1306.5	17	1039.2	17
C=Ti str	818.9	117	818.6	116	806.0	119	707.9	55
TiH_2 bend	689.2	17	689.0	16	683.6	12	572.6	19
CH_2 wag	675.0	200	681.8	16	675.6	212	537.5	147
TiH_2 rock	532.4	15	532.0	18	529.2	17	407.1	14
CH_2 twist	476.9	3	506.5	3	505.7	4	360.8	0
CH_2 rock	311.1	9	297.7	8	297.3	8	213.9	4
TiH_2 wag	85.3	337	33.4	356	33.4	356	24.0	189

[a] Calculated with 6-311++G(3df,3pd) basis. [b] Infrared intensities (km/mol). [c] Calculated with 6-311++G(2d,p).

Table 3. Harmonic Vibrational Frequencies (cm^{-1}) Calculated for $(CH_3)_2TiH_2$ Isotopic Molecules Using the B3LYP Density Functional

mode	$(CH_3)_2TiH_2$	$(CH_3)_2TiH_2$	$(^{13}CH_3)_2TiH_2$	$(CD_3)_2TiD_2$
Ti−H_2 str	1715.4 (292)[a]	1744.7 (284)[b]	1715.4 (1292)[a]	1221.8 (159)[a]
Ti−H_2 str	1683.8 (454)	1711.7 (448)	1683.8 (454)	1209.4 (240)
CH_2 bend	1411.3 (13)	1411.0 (11)	1408.2 (13)	1024.7 (9)
C−H_2 bend	1410.7 (19)	1410.5 (18)	1407.3 (19)	1025.4 (12)
CH_3 def	1134.7 (12)	1138.5 (12)	1123.9 (9)	908.6 (40)
C−Ti str, Ti−H_2 bend	616.8 (230)	627.9 (214)	612.4 (227)	524.2 (141)
C−Ti str, Ti−H_2 bend	614.8 (130)	629.9 (116)	612.4 (127)	510.0 (52)
Ti−H_2 def	467.8 (25)	465.7 (20)	464.4 (25)	423.1 (24)

[a] All-electron 6-311++G(2d, p) basis. [b] 6-311++G(3df, 3pd) for C and H and SDD for Ti.

Table 4. Vibrational Frequencies (cm^{-1}) Calculated for $CH_3{-}TiH$[a]

approx mode	$^{12}CH_3{-}TiH$	$^{13}CH_3{-}TiH$	$CD_3{-}TiD$
C−H stretch	3073.3 (6)	3062.8 (6)	2271.2 (2)
C−H stretch	3035.9 (12)	3025.4 (13)	2243.0 (4)
C−H stretch	2970.0 (7)	2966.9 (8)	2128.8 (1)
Ti−H stretch	1577.9 (430)	1577.9 (429)	1128.2 (225)
C−H_2 bend	1425.0 (2)	1421.8 (2)	1034.2 (2)
C−H_2 bend	1416.1 (1)	1412.9 (1)	1028.0 (1)
C−H bend	1135.9 (5)	1126.3 (4)	895.3 (18)
C−Ti−H bend	556.4 (128)	550.6 (125)	470.7 (81)
C−Ti stretch	457.2 (9)	449.2 (9)	372.0 (7)
CH_3 motion	384.2 (20)	382.2 (19)	288.4 (14)
CH_3 motion	301.7 (40)	301.4 (40)	216.1 (22)
CH_3 motion	165.4 (56)	165.3 (56)	118.1 (30)

[a] B3LYP, all-electron 6-311++G(3df, 3pd) basis.

14 kcal/mol higher in energy with a longer C−Ti bond (2.070 Å), equivalent C−H bonds (1.095 Å, CH_2 angle 110.4°, H−C−Ti angle 124.8°) and equivalent Ti−H bonds (1.749 Å, TiH_2 angle 117.7°, H−Ti−C angle 121.2°) using the medium basis set.

The singlet $CH_2{=}TiH_2$ calculation was repeated using the BPW91 density functional[19] and large basis set, and the distorted structure is almost the same as in Figure 5 for the B3LYP functional (BPW91: C=Ti, 1.816 Å; H−C−Ti angle 88.7°; C−H, 1.126, 1.092 Å; Ti−H, 1.742 Å, 1.755 Å). The MP2 method[19] and large basis set gave a more distorted minimum energy C_s structure (MP2: C=Ti, 1.799 Å; H−C−Ti angle 78.5°; C−H, 1.134 Å, 1.082 Å; Ti−H, 1.748 Å, 1.776 Å). When the structure was fixed at C_{2v}, the MP2 calculation found a longer C=Ti bond (1.821 Å), an H−C−Ti angle (120.1°) appropriate for sp^2 hybridization, an imaginary CH_2 in-plane deformation frequency (i 339 cm^{-1}), and 3.2 kcal/mol higher energy. Clearly this planar symmetrical "transition state" can distort the CH_2 group to attain the lower energy C_s structure that is stabilized by the agostic bonding interaction. Finally, a CCSD calculation with the large basis set also gave a planar distorted structure (CCSD: C=Ti, 1.852Å; H−C−Ti angle 89.6°; C−H, 1.120Å, 1.089Å; Ti−H, 1.767Å, 1.772Å).

The $CH_2{=}TiH$ radical doublet ground-state structure, also shown in Figure 5, is 8 kcal/mol lower than the quartet state. The doublet methylidene hydride radical has a slightly longer C=Ti double bond than $CH_2{=}TiH_2$ itself and retains the CH_2 distortion: the Ti−H stretching frequency is computed as 1577 cm^{-1}. The $CH_2{=}TiH^-$ anion triplet ground state (not shown) has a longer C−Ti bond (1.887 Å) and agostic H−C−Ti angle (83.9°) with the medium basis set: the Ti−H stretching frequency is computed as a very strong band at 1325 cm^{-1}. Finally, the doublet $CH_2{=}TiH_2^-$ anion is stable by 36 kcal/mol, and it has longer Ti−H bonds (1.835, 1.847 Å) and C=Ti bond (1.883 Å), H−C−Ti angle (88.7°) and two very strong Ti−H stretching modes at 1373 and 1396 cm^{-1} (medium basis set).

The most intense infrared absorptions computed for $(CH_3)_2TiH_2$ are given in Table 3 for all-electron calculations using the 6-311++G(2d,p) basis set. The all-electron frequency calculation would not converge with the 6-311++G(3df,3dp) basis set, but with SDD for Ti, this calculation gave the 2−28 cm^{-1} higher frequencies listed in Table 3. Like CH_3ZrH, CH_3TiH is a "one-band" molecule as only the intense Ti−H stretching mode computed at 1577.8 cm^{-1} (350 km/mol) using the large basis for all electrons for the triplet ground-state molecule[16] has observable intensity. All computed frequencies for CH_3TiH are listed in Table 4. Finally, Mulliken charges for the five species in Figure 5 are listed in Table 5.

For comparison calculations were done for TiH_2 and TiH_4. At the B3LYP level the $^3A_2$ ground state (1.782 Å, 122.8°) gave 1587 cm^{-1}, a_1, 144 km/mol and 1525.3 cm^{-1}, b_2, 633 km/mol, and 486 cm^{-1}, a_1, 251 km/mol for TiH_2. Computations for TiH_4 were obtained (1787 cm^{-1}, a_1, 0 km/mol; 1732 cm^{-1}, t_2, 435 × 3; 615 cm^{-1}, e, 0 × 2; 525 cm^{-1}, t_2, 144 × 3, Ti−H, 1.698 Å). Mulliken charges were obtained for the binary hydrides TiH_2 (0.68, −0.34) and TiH_4 (1.143, −0.286).

Table 5. Mulliken Charges Calculated[a] for the C, H, and Ti Species in Figure 5

atom	$CH_2=TiH_2$	$CH_2=TiH$	CH_2Ti	CH_3TiH	$(CH_3)_2TiH_2$
C	−0.47	−0.50	−0.39	−0.37	−0.44
H_1	0.08	0.06	0.040	0.01	−0.24
H_2	0.06	0.04	0.038	−0.001	0.02
Ti	0.91	0.70	0.31	0.69	1.25
H_3	−0.27	−0.30		−0.001	0.02
H_4	−0.31			−0.32	0.01

[a] B3LYP, all-electron 6-311++G(3df,3pd) basis.

Discussion

The molecular products of methane activation by Ti will be identified from matrix infrared spectra and DFT calculations.

CH_3TiH. The first product anticipated is the titanium-inserted CH_3-Ti-H species, which has been characterized by a weak 1513.5 cm^{-1} absorption following 500 nm irradiation of argon/Ti/CH_4 samples and density functional calculations of a stable triplet ground state with a strong Ti−H stretching mode at 1551 cm^{-1}.[16] Our experiments and calculations (1578 cm^{-1} Ti−H mode) are in agreement with the work with Bihlmeier et al. We also observe several matrix sites of this species at 1516.8, 1513.5, 1508.7, and 1503.3 cm^{-1} (Figure 1, labeled **in** for insertion product) owing to our different method of synthesis. We have more isotopic data: the strong absorptions show no $^{13}CH_4$ shift, as expected for the Ti−H stretching mode, and no shift with CH_2D_2, as there is no coupling with methyl H(D) through Ti in the CHD_2-Ti-H isotopic molecule. We also observed this species in solid neon at 1541.4 cm^{-1}, which is a reasonable matrix shift from 1513.5 cm^{-1} for a triplet state organometallic species with some dispersive matrix interaction.[25] This frequency for the divalent Ti species CH_3TiH may be compared to the 1549.1 cm^{-1} value recently observed for HOTiH.[23] In addition, we employed different irradiations and found that CH_3-Ti-H undergoes persistent photoreversibility with a product responsible for new 1560.0 and 1553.1 cm^{-1} absorptions not observed previously. These new absorptions will be assigned next to the titanium methylidene dihydride complex.

$CH_2=TiH_2$. The new 1560.0 and 1553.1 cm^{-1} absorptions (labeled **m**) are weak on sample deposition, but they increase at least 3-fold on near-ultraviolet 290−380 nm irradiation. Subsequent visible $\lambda > 420$ nm irradiation reduces the **m** bands and increases the **in** bands, and the next 290−380 nm irradiation restores the **in** bands at the expense of the **in** absorption (Figure 1b−d). Similar photochemical behavior was found for the CH_3TiX and $CH_2=TiHX$ species (X = F, Cl, Br),[10,13] and accordingly calculations were performed to predict the spectrum of $CH_2=TiH_2$. The calculations given in Table 2 find two strong TiH stretching frequencies at 1673.5 and 1631.7 cm^{-1}, namely symmetric and antisymmetric $Ti-H_2$ stretching modes, and the latter is 54 cm^{-1} above the strong absorption calculated for CH_3TiH. The 1560.0 cm^{-1} **m** band is 51.3 cm^{-1} above our strongest CH_3TiH absorption at 1508.7 cm^{-1}. The H/D ratio 1560.0/1132.2 = 1.378 is appropriate for a Ti−H(D) stretching mode. The **m′** band is due to a different argon matrix packing configuration. This Ti−H stretching mode may be compared with the 1602.8 cm^{-1} value observed for $CH_2=TiHF$.[10] The weak 1598.1 cm^{-1} absorption is in agreement with the prediction of higher frequency, weaker Ti−H stretching modes.

Our calculations find agostic distortion at CH_2 (Figure 5), and this should be manifest in the strongest Ti−H(D) stretching mode in the mixed $CHD=TiHD$ isotopic molecules. Four such mixed isotopic molecules have been described for agostic $CHD=ZrHD$,[8] and these $CHD=TiHD$ molecules (Chart 1) exhibit slightly different Ti−H(D) stretching frequencies from $CH_2=TiH_2$ and $CD_2=TiD_2$. Hence, the agostic distortion (inequivalent hydrogen atoms) will produce different Ti−H(D) stretching modes for the four $CHD=TiHD$ molecules. Our calculations predict that isomers 3 and 5 will have a Ti−H stretching mode up 29.7 and 29.5 cm^{-1} from $CH_2=TiH_2$ and isomers 4 and 6 up 13.5 and 13.6 cm^{-1}. We observe new bands (arrows in Figure 3b) up 13 cm^{-1}, and up 30 cm^{-1} is covered by water absorption. Similarly isomers 3−6 are predicted to have Ti−D stretching modes up 1.4, 18.6, 7.0, and 12.3 cm^{-1}, and we observe new bands up 5.1 and 11.6 cm^{-1}. Thus, we have clearly identified isotopic molecules 4, 6 and 3, 5 from new Ti−H stretching modes and 5, 6 from new Ti−D stretching modes. On the other hand, the symmetrical planar $CHD=TiHD$ molecule would have Ti−H and Ti−D stretching modes up 20.9 and 9.8 cm^{-1} from the strongest bands of $CD_2=TiH_2$ and $CH_2=TiD_2$, respectively, and this is not observed. These $CHD=TiHD$ observations are sufficient to support experimental characterization of agostic $CH_2=TiH_2$. Finally, our MP2 calculation finds a 3.2 kcal/mol higher energy planar symmetrical stationary state, which separates two equivalent agostic minimum energy structures characterized here.

Our calculations also predict that a third mode, the out-of-plane $C-H_2$ wag, at 675.0 cm^{-1} should be observable, and our weak 635.7 cm^{-1} absorption with matching photochemical behavior is appropriate for such a vibration. The observed H/D ratio 635.7/514.0 = 1.237 is also in good agreement with the 1.268 value calculated for this mode. The 1598.1, 1560.0, and 635.7 cm^{-1} bands are accordingly assigned to the new molecule $CH_2=TiH_2$, which is similar to the recently reported $CH_2=ZrH_2$ counterpart.[8]

There is no apparent neon matrix absorption for $CH_2=TiH_2$ as this species seems to react readily with methane to give the $(CH_3)_2TiH_2$ secondary reaction product.

$(CH_3)_2TiH_2$. Annealing the sample to 26 K markedly increased new absorptions at 1636.5 and 1618.2 cm^{-1}

---

(25) Jacox, M. E. *Chem. Phys.* **1994**, *189*, 149.

Chart 1

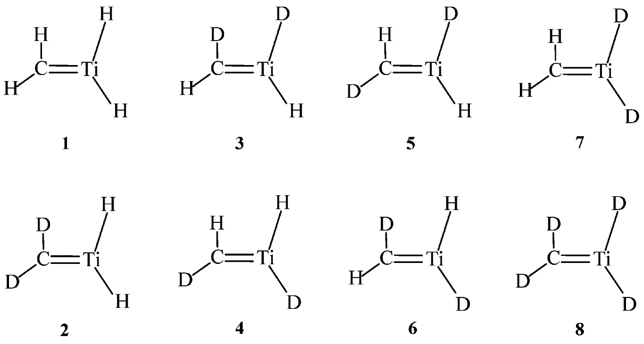

(labeled **di** for dimethyltitanium dihydride), which increased together on ultraviolet (240−380 nm) irradiation to give more increase in CH_3TiH than $CH_2{=}TiH_2$ absorption. Similar annealing behavior has been observed in CH_3X reactions with Ti; new absorptions were identified as $(CH_3)_2TiX_2$ (X = F, Cl, Br),[10,13,14] and the new molecule $(CH_3)_2TiH_2$, analogous to $(CH_3)_2ZrH_2$,[8] is expected. The marked increase in the **di** absorptions relative to **m** and **in** on increasing CH_4 concentration supports this hypothesis.

Isotopic observations show that the 1636.5 and 1618.2 cm^{-1} bands are Ti−H stretching modes, namely no $^{13}CH_4$ shift and H/D ratios 1.389 and 1.378 for symmetric and antisymmetric $Ti{-}H_2$ stretching modes.[26] In the CH_2D_2 reaction, new intermediate bands at 1627.2 and 1176.7 cm^{-1} are for the simple Ti−H and Ti−D stretching modes that result from the $(CH_2D)(CHD_2)TiHD$ product. Note that more $(CHD_2)_2TiH_2$ appears to be observed than $(CH_2D)_2TiD_2$ as the upper 1636.7, 1618.1 cm^{-1} $Ti{-}H_2$ absorptions are more than twice as strong as the lower 1179.4, 1173.9 cm^{-1} $Ti{-}D_2$ bands.

The neon matrix counterparts at 1657 and 1637 cm^{-1} are blue shifted by 20 and 19 cm^{-1}, which indicates a weaker matrix interaction for the singlet $(CH_3)_2TiH_2$ species than the triplet CH_3TiH molecule. The analogous $Ti^{IV}H_4$ molecule shows a similar but typical[25] 1686.1 − 1663.8 = 22.3 cm^{-1} neon-to-argon matrix shift.[27,28] The higher yield of **di** relative to **in** absorptions in neon experiments arises from the slower condensation rate of neon at 4 K compared to argon at 8 K, which promotes additional secondary CH_4 reactions in neon.

B3LYP calculations (Table 3) predict three strong absorptions for $(CH_3)_2TiH_2$, namely symmetric and antisymmetric $Ti{-}H_2$ stretching modes at 1715.4 and 1683.8 cm^{-1} and an antisymmetric $Ti{-}C_2$ stretching, $Ti{-}H_2$ deformation vibration at 616.8 cm^{-1}. The $Ti{-}H_2$ stretching modes are predicted 41.9 and 52.1 cm^{-1} higher for $(CH_3)_2TiH_2$ than for $CH_2{=}TiH_2$, and the **di** bands are observed 38.4 and 58.2 cm^{-1} higher than the **m** bands, which is excellent agreement between experimental observation and theoretical prediction. Furthermore the scale factors (observed/calculated frequencies) for the five Ti−H modes assigned here CH_3TiH(0.959), $CH_2{=}TiH_2$(0.955, 0.956), and $(CH_3)_2TiH_2$ (0.938, 0.945) are typical of B3LYP calculations for transition metal compounds.[30] The $Ti{-}C_2$ stretching, $Ti{-}H_2$ bending mode predicted at 616.8 cm^{-1} is observed at 588.5 cm^{-1} (scale factor 0.954), and this mode has a H/D = 588.5/510.0 = 1.154 ratio. The isotopic data and frequency calculations confirm the identification of dimethyltitanium dihydride. Methyltitanium compounds are of interest as catalysts, and several structures have been recently investigated.[31]

The only binary titanium hydride molecules known are TiH_2 (1435.5 cm^{-1}) and TiH_4 (1663.8 cm^{-1}) in solid argon.[27−29] The strong antisymmetric Ti−H stretching mode in $Ti^{IV}H_4$ is higher than that in $(CH_3)_2Ti^{IV}H_2$ as predicted at 1732 cm^{-1} by B3LYP calculation with the large basis set. We observe no TiH_4 product in these reactions with CH_4, but a weak TiH_2 band is observed. Finally, the two $Ti{-}H_2$ stretching frequencies for the tetravalent Ti species $(CH_3)_2TiH_2$ in solid argon at 1636.5 and 1618.2 cm^{-1} are slightly lower than those found recently for $(HO)_2TiH_2$ at 1688.3 and 1666.2 cm^{-1}.[23]

The ultraviolet photolysis that forms $(CH_3)_2TiH_2$ in solid neon also produces two absorptions at 1456 and 1437 cm^{-1}, which sharpen on annealing to 1453.5 and 1433.7 cm^{-1}. These bands are observed unshifted with $^{13}CH_4$, and the stronger band shifted to 1047.3 cm^{-1} with CD_4 (H/D ratio 1.3879). With CH_2D_2, two sharp bands were observed at 1462.3 and 1055.0 cm^{-1}, just above the CH_4 and CD_4 product absorptions. This new band appears to be due to a TiH_2 vibration, which appears just above TiH_2 in solid argon, but our neon matrix reactions with Ti and H_2 failed to trap TiH_2.[27−29] These bands appear to be due to triplet TiH_2 trapped here most likely as a complex with ethane. Such a complex could result from a side decomposition reaction in the formation of $(CH_3)_2TiH_2$.

Agostic Bonding. The methylidene dihydride complex provides a simple subject for examination of the agostic bonding phenomenon particularly in view of two recent excellent review articles.[32,33] Our B3LYP calculations using the large Gaussian basis set with four polarization functions on each atom clearly show distortion of the CH_2 and TiH_2 subgroups in planar singlet $CH_2{=}TiH_2$, but the C═Ti bond stabilization cannot be easily quantified for want of a standard comparison. On the basis of the methylene distortion as measured by the computed H−C−M angle, we find more agostic distortion in $CH_2{=}TiH_2$ (angle 91.4°) than in $CH_2{=}ZrH_2$ (angle 92.9°),[8] and in $CH_2{=}HfH_2$ (angle 95.6°).[9] From the early description of the agostic bonding interaction, we expect C−H bond coordination to an electron deficient

---

(26) The **G** matrix elements for symmetric and antisymmetric modes of a MH_2 group are different: $G_{sym} = \mu H + \mu M + \mu M \cos \alpha$ and $G_{antisym} = \mu H + \mu M - \mu M \cos \alpha$, where μ is the reduced (i.e. inverse) mass. Thus for $90° < \alpha < 180°$, the sym mode has less metal and hence more H participation.

(27) Xiao, Z. L.; Hauge, R. H.; Margrave, J. L. *J. Phys. Chem.* **1991**, *95*, 5, 2696.

(28) Chertihin, G. V.; Andrews, L. *J. Am. Chem. Soc.* **1994**, *116*, 8322.

(29) Analogous experiments with Ti and H_2 in excess neon gave a sharp 1686.1 cm^{-1} absorption for TiH_4, but no TiH_2 appeared to be trapped.

(30) Bytheway, I.; Wong, M. W. *Chem. Phys. Lett.* **1998**, *282*, 219.

(31) Kleinhenz, S.; Seppelt, K. *Chem.*−Eur. J. **1999**, *5*, 3573.

(32) Scherer, W.; McGrady, G. S. *Angew. Chem., Int. Ed.* **2004**, *43*, 1782.

(33) Clot, E.; Eisenstein, O. Agostic Interactions from a Computational Perspective. In *Structure and Bonding, Computational Inorganic Chemistry*; Kaltzoyannis, N., McGrady, J. E., Eds.; Springer-Verlag: Heidelberg, Germany, 2004; pp 1−36,

transition metal center.[34,35] However, is CH_2 distortion the cause or the effect of C═M bond stabilization or does the CH_2 subunit deform to stabilize the C═M bond? The two appear to go hand-in-hand in the series $CH_2{=}TiHX$ (X = F, Cl, Br) where the H−C−Ti angle decreases and the C═Ti bond length decreases down the family series.[10,13] There is no agostic distortion in triplet $CH_2{-}TiH_2$ and $CH_3{-}Ti{-}H$ nor singlet $(CH_3)_2TiH_2$, which have considerably longer single C−Ti bonds (Figure 5).

We computed the methylidene hydride radical and the titanium carbene just for this comparison: the doublet ground-state radical retains the C═Ti double bond and agostic bonding. The triplet ground-state carbene has a single C−Ti bond and very little distortion of the CH_2 subgroup (Figure 5). Even the 18 kcal/mol higher energy singlet $CH_2{-}Ti$ molecule is symmetrical with C_{2v} symmetry, C−Ti = 1.896 Å, C−H = 1.092 Å, and H−C−Ti = 122.0°. Although Mulliken charges probably overestimate the actual charge distribution in the molecule, the comparison of ground-state singlet $CH_2{=}TiH_2$ and triplet $CH_2{-}Ti$ (Table 5) shows that the additional H_3 and H_4 attract negative charge, increase positive charge on the Ti center, and stabilize the carbon−titanium bond, which allows distortion of the CH_2 subgroup in singlet $CH_2{=}TiH_2$. The only molecules that exhibit agostic bonding contain a short C═Ti double bond. In this regard it is perhaps not surprising that $CH_3{-}TiCl_3$ with a long C−Ti bond (2.05 Å) appears after thorough investigation to exhibit no agostic interaction.[31,36]

Reactions Occurring in the Matrix. The primary reaction is insertion to form CH_3TiH, which is exothermic ($\Delta E = -14$ kcal/mol, B3LYP all electron, large basis) but requires activation by laser ablation or photoexcitation.[16] We find that irradiation at 290−380 nm, where Ti atoms in solid argon exhibit strong absorptions,[37] markedly increases the $CH_3{-}TiH$ product absorption. The energized triplet CH_3TiH intermediate can be relaxed by the matrix, reaction 1, or undergo α-H transfer to the triplet methylidene, which can be relaxed to the singlet methylidene ground state, reaction 2. Both triplet $CH_3{-}TiH$ and singlet $CH_2{=}TiH_2$ can in principle activate methane to give the dimethyltitanium dihydride, reaction 3. Both appear to give way on annealing to 26 K in solid argon and form $(CH_3)_2TiH_2$. Although $CH_2{=}TiH_2$ is not detected in solid neon, this reactive molecule could activate methane instead of being isolated in the softer neon matrix.

$$Ti^* + CH_4 \rightarrow [CH_3TiH]^* \xrightarrow{\text{relax}} CH_3TiH \qquad (1)$$

$$Ti^* + CH_4 \rightarrow [CH_3TiH]^* \rightarrow [CH_2\text{-}TiH_2]^* \xrightarrow{\text{relax}} CH_2{=}TiH_2 \qquad (2)$$

$$CH_3TiH \text{ or } CH_2{=}TiH_2 + CH_4 \rightarrow (CH_3)_2TiH_2 \qquad (3)$$

The reversible photochemistry of CH_3TiH and $CH_2{=}TiH_2$ is reminiscent of the CH_3TiX and $CH_2{=}TiHX$ cases.[10,13] Here triplet CH_3TiH is excited in the near-ultraviolet through a triplet excited state to triplet $CH_2{-}TiH_2$, which intersystem crosses to the lower energy ground singlet methylidene $CH_2{=}TiH_2$. The lowest triplet state of $CH_2{-}TiH_2$ is 14 kcal/mol higher energy than the singlet $CH_2{=}TiH_2$ ground state. Then singlet $CH_2{=}TiH_2$ is excited in the visible through a singlet excited state to singlet CH_3TiH, which intersystem crosses to the lower energy triplet ground state. The CH_3TiH(T) state is 22 kcal/mol lower (all electron, large basis) in energy than the $CH_2{=}TiH_2$ (S) methylidene complex. Accordingly reaction 3 is 22 kcal/mol more exothermic starting with $CH_2{=}TiH_2$, which gives a total $\Delta E = -37$ kcal/mol at the B3LYP all-electron 6-311++G(2d,p) level.

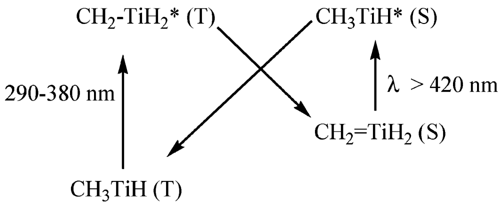

(4)

Conclusions

Titanium atoms when excited react with methane to form the insertion product methyltitanium hydride CH_3TiH, which undergoes a reversible photochemical α-H transfer to give the methylidene dihydride complex $CH_2{=}TiH_2$. On annealing a second methane activation occurs to produce $(CH_3)_2TiH_2$. These molecules are identified by isotopic substitution (CH_4, $^{13}CH_4$, CD_4, CH_2D_2) and comparison to DFT frequency calculations. The computed planar structure for singlet ground-state $CH_2{=}TiH_2$ shows CH_2 distortion and evidence for agostic bonding (B3LYP, angle H−C−Ti, 91.4°). The symmetrical planar stationary state is 3.2 kcal/mol higher in energy (MP2) and has an imaginary CH_2 in-plane deformation mode, which leads to distortion and stabilization through agostic bonding. This agostic distortion is verified experimentally through the observation of IR bands for cis and trans CHD═TiHD isomers that are different from that calculated for the cis and trans isomers for the symmetrical nonagostic molecule.

Acknowledgment. We gratefully acknowledge financial support from NSF. Grants CHE 00-78836 and CHE 03-52487, sabbatical leave support (H.-G.C.) from the Korea Research Foundation (Grant KRF-2003-013-C00044), and helpful correspondence with G. S. McGrady and O. Eisenstein.

IC0502574

---

(34) Brookhart, M.; Green, M. L. H. *J. Organomet. Chem.* **1983**, *250*, 395.

(35) Brookhart, M.; Green, M. L. H.; Wong, L. L. *Prog. Inorg. Chem.* **1988**, *36*, 1.

(36) McGrady, G. S.; Downs, A. J.; Bednall, N. C.; McKean, D. C.; Thiel, W.; Jonas, V.; Frenking, G.; Scherer, W. *J. Phys. Chem. A* **1997**, *101*, 1951 and references therein.

(37) Gruen, D. M.; Carstens, D. H. W. *J. Chem. Phys.* **1971**, *54*, 5206.